Optics & Laser Technology 146 (2022) 107602

Contents lists available at ScienceDirect

Optics and Laser Technology

journal homepage: www.elsevier.com/locate/optlastec

Improvement of high-order harmonics from silver plasma plumes induced by femtoseconds laser pulses

Srinivasa Rao Konda [a,*], Yu Hang Lai [a], Wei Li [a,b,*]

[a] GPL, State Key Laboratory of Applied Optics, Changchun Institute of Optics, Fine Mechanics and Physics, Chinese Academy of Sciences, Changchun 130033, China
[b] University of Chinese Academy of Sciences, Beijing 100049, China

ARTICLE INFO

Keywords:
Silver plasma plumes
Chirped pulses
HHG
Fs pulses
Laser-induced plasma

ABSTRACT

Silver plasma plume is one of the potential sources for high-order harmonics generation (HHG) using a driving pulse of 800 nm (Ti: S laser system). The harmonic intensity (yield) and cut-off are significantly affected by ablating laser pulse duration. This work extended the harmonics generation using silver [bulk and nanoparticles (100 nm and 20 nm)] plasma plumes ablated by fs laser pulses. The shorter pulse duration of fs pulses leads to enhanced ions' density, which improves the harmonics' intensity and cut-off (65H). Moreover, the experimental harmonic cut-off for Ag^{+} is precisely matched with the theoretical cut-off. In Ag^{2+} ions, the experimental cut-off is ~1.3 times less than the theoretical cut-off. In addition, we have measured the harmonic spectra of samples using negatively and positively chirped 135 fs driving pulses and compared them with chirp-free 35 fs driving pulse harmonic spectra. The negative and positive chirps of the pulses lead to blueshift and redshift of the harmonic's spectra, with an increase of intensity of low (9H–15H) and higher (17H–41H) range harmonics, respectively. However, the comparison between bulk and nanoparticles (NPs) studies proved that the smallest NPs possess larger HHG efficiency. The present study highlights the selection of short pulse duration, i.e., fs pulses as driving and ablating laser pulses, for enhancing the yield and cut-off of harmonics for next-generation table-top XUV light sources.

1. Introduction

High harmonic generation (HHG) from laser-induced plasma (LIP) plumes created from solid materials have been widely studied over the past decade [1–8]. The efficiency and cut-off photon energy of emitted harmonics varied significantly based on different materials, also depended on the plasma plumes characteristics [9–15]. The ablating laser parameters (wavelength, pulse duration, energy) and ambient environmental conditions significantly influence the plasma plume characteristics. In our earlier work, we have demonstrated the HHG from silver plasma ablated by ns and ps pulses [16]. In the present report, for the first time, we have shown the advantages of fs heating pulses (HP) to create the plasma plumes in terms of intense high order harmonics with higher cut-off than ns/ps HPs reported in earlier studies [17–21]. The fluence we used for ns, ps (in our earlier work [16]) and fs (current work) is almost similar. However, the ablation intensities of these pulses have differed from the $1:10^{3}:10^{6}$ ratio. But the higher cut-off and intense harmonics were achieved in the case of plasma plume produced by fs pulses (fs LIPs) due to the high density of plasma components.

Verhoff et al. showed that the fs LIP extension dynamics are expressively changed, i.e., having a narrower angular distribution of ions and evaporated mass than ns LIP [22]. The expansion length for fs LIP is 10 mm, whereas it is limited to 2.5 mm for ns LIP. Similarly, for ps, plasma expansion angle can be smaller (volume is less, i.e., density is increased) and having a narrower angular distribution of ions than the ns LIPs. Therefore, the order of density of plasma plumes (having a higher number of ions) is expected to be fs LIPs > ps LIPs > ns LIPs. A similar order was achieved for harmonics cut-off and intensities in the present and earlier work [16].

The present report estimated the Ag^{+} and Ag^{2+} contribution in measured HHG spectra obtained from fs LIPs. The attained harmonics intensity and cut-off were compared with ps LIPs for silver bulk and nanoparticles (NPs). In both fs LIPs and ps LIPs cases, we measured the harmonics spectra of silver at driving pulse (DP) intensity between 0.6 and 4.8×10^{14} W/cm^{2} range. In the case of fs LIPs, the experimentally

* Corresponding authors at: GPL, State Key Laboratory of Applied Optics, Changchun Institute of Optics, Fine Mechanics and Physics, Chinese Academy of Sciences, Changchun 130033, China.
E-mail addresses: ksrao@ciomp.ac.cn (S.R. Konda), weili1@ciomp.ac.cn (W. Li).

https://doi.org/10.1016/j.optlastec.2021.107602
Received 25 August 2021; Received in revised form 6 October 2021; Accepted 11 October 2021
Available online 20 October 2021

obtained cut-off is matched with Lewenstein model simulations and classical calculations from Ag atom, Ag^{+}, and Ag^{2+} ions reported in Ref [16]. In addition, we have shown the effect of positive and negative chirps of DP on the emission of higher-order harmonics. Earlier, several research groups reported the HHG from various materials (solids), LIPs, and gas jets [23–32]. In particular, Ganeev et al. demonstrated the HHG from Ag plasma using chirp-free 48 fs and chirps from −165 fs to +260 fs ('−' and '+' sings corresponding to negative and positive chirps, respectively) and shown the corresponding shifts of 47H [33]. In this case, they created the silver plasma plumes using 300 ps pulses. However, in this work, we demonstrated the HHG studies using DP of chirp-free 35 fs and negatively (−) and positively (+) chirped 135 fs pulses using corresponding fs laser pulses as HPs.

Earlier researchers have explored the different sizes of NPs for HHG studies ablated by ns and ps laser pulses. Here, we would like to clarify and elaborate on the motivation to select specific sizes of NPs in this report (i.e., the comparison between bulk Ag and NPs). Over the last few years, HHG in the LIPs generated from different NPs have been studied (e.g., the review article [34] and the references therein). Some studies found that one main advantage of using NPs is that they give higher HHG yields [21]. However, in some other works, it was found that the HHG yield from bulk solid was higher [20]. Earlier studies also demonstrated that the lowest NPs possess better efficiency of harmonics. Therefore, to clarify the above peculiarities, we have selectively chosen the commercially available Ag (purity > 99.95%) NPs powders of smaller size with 20 nm and results are compared for bulk and five times larger NPs (100 nm), respectively. Overall, the present report reveals the advantages of shorter pulse durations (fs pulses) to create the plasma plumes for the promising potential application for the next generation of table-top XUV light sources [35–39].

2. Experimental details

Fig. 1(a) shows the schematic layout for the HHG setup. Ti: S laser system (Spectra-Physics) provides 800 nm, 35 fs, 1 kHz laser pulses. The HHG measurements were carried out at a 300 Hz repetition rate because, at 1 kHz, the harmonics spectra rapidly saturate in the case of fs LIPs. We have used chirp-free 35 fs pulses and ±135 fs pulses as the driving laser beams. The chirped pulse was obtained by changing the distance between compression gratings. The pulse duration (τ_p) was confirmed by autocorrelator (PulseScout PSCOUT2-NIR-PD, Spectra-Physics). The negatively (−) and positively(+) chirped pulses have similar spectral components with chirp-free 35 fs pulses, but they possess temporal broadening. The spectral distribution of chirp-free 35 fs pulses and ±135 fs chirped pulses are shown in Fig. 1(b), which confirms that the chirp of laser pulses does not affect the central wavelength.

In the XUV region, the HHG spectra between 10 and 100 nm range were collected using the same XUV spectrometer as in [16,40]. The LIP is created by ablating the target with identical laser pulses as HPs in the first vacuum chamber (Target Chamber). The delay between DP and HP was fixed at 80 ns by extending the path length of DP using additional optical mirrors. The targets consist of bulk silver (99.99% Ag, DK Nano, China) with a 1 mm thickness of 10 mm × 10 mm. The NPs sample target was made like a pellet of diameter 10 mm and thickness 1 mm by a simple compression method without mixing with other substances. This method ensures the ablated plasma plume is free of unwanted substances from the polymers.

The emitted harmonics from LIPs of the target were allowed to the second vacuum chamber (XUV chamber) by passing through a narrow slit (controlled by vertical and horizontal axes and opened for ~2 mm) which maximum blocks the fundamental radiation and a large amount of incoherent plasma. The XUV chamber consists of gold-coated cylindrical mirror (CM), flat-field grating (FFG) [1200 grooves/mm, Hitachi] and microchannel plate (MCP) to guide the harmonics. After passing through the slit, the harmonics were directed to fall on CM and reflected to FFG. The MCP (in XY plane) was placed perpendicular to the FFG (in ZY plane), which provides the focused image translation of dispersed harmonics along the plane to obtained the sharp image of harmonics distribution along with the whole spectral range and the fundamental

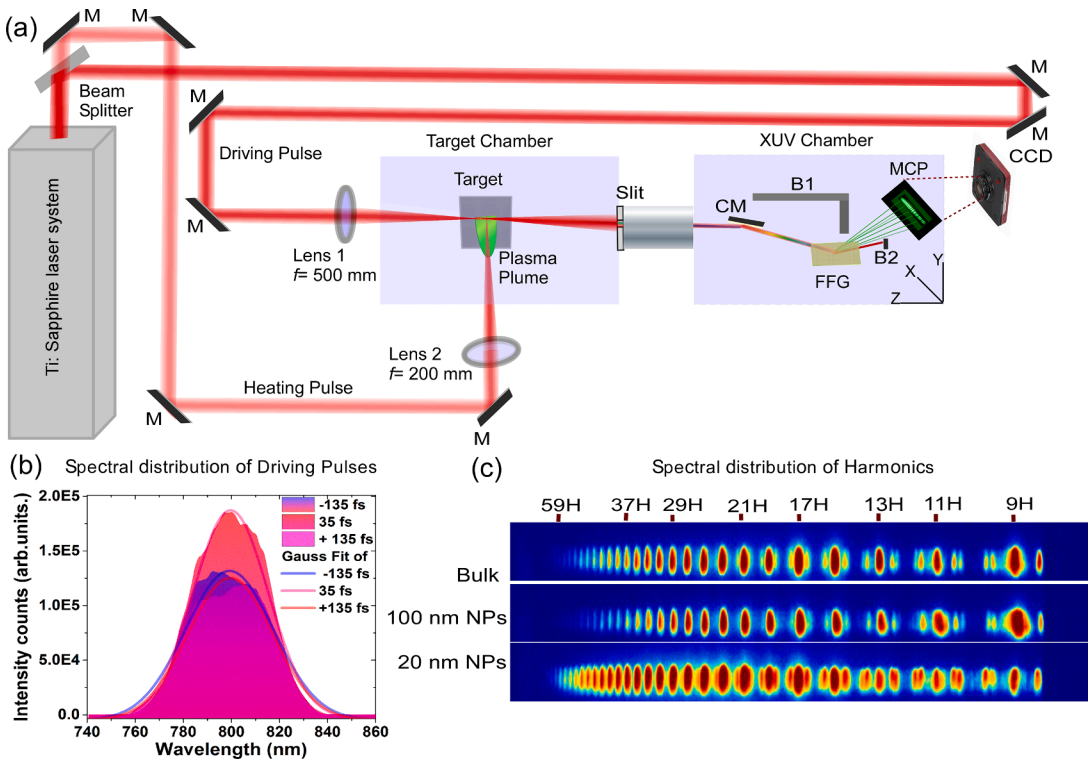

Fig. 1. (a) Experimental setup. T: Ag bulk, NPs (100 nm, 20 nm), (b) the spectral distribution of driving pulses, and (c) the spectral distribution of harmonics for bulk and NPs at $I_{DP} = 4.8 \times 10^{14}$ W/cm^2, $I_{HP} = 6.2 \times 10^{14}$ W/cm^2.

beam was blocked with blocker B2. Finally, the HHG spectra were collected using the charge-coupled device (CCD) camera, placed outside the XUV chamber.

The ultrashort laser pulses create a crater during the ablation of metal targets. The depth will be high in the case of fs laser ablation [41]. During the HHG measurements, we have recorded ten spectra for one set of data and presented the average of them. Depending on the intensity of HP (I_{HP}), the surface of the targets emits a bright plasma plume while the DP propagates through it and emits the harmonics. Initial few shots of ablation intense harmonics are obtained, further ablating on the same position signal is lost. Because the focus position is changed and a high intense ablating laser pulse damages material. Therefore, it is necessary to expose the HP to the new surface of the target; for this, we have moved the sample in a vertical direction to collect the next set of data.

We have observed the incoherent plasma emission during the ablation of targets using fs pulses with the fluency of 21.7 J/cm^2. However, by controlling the slit width, most incoherent plasmas were blocked, and the remaining plasma, along with harmonics, entered the XUV chamber. Further, the incoherent plasma is secured by keeping the extra blocker (B1) behind the gold-coated cylindrical mirror is shown in Fig. 1(a). This blocker also stops the scattering of light from flat-field grating. After taking these precautions, the intensity of harmonics is much stronger than the incoherent plasma, which is slightly visible in the background of measured harmonics spectra. Meanwhile, the HHG spectra also consist of a little stronger second-order diffraction patterns from the grating. In the case of 20 nm NPs spectra, these diffraction patterns are visible between 9H and 27H, and two spots surround each harmonic, as shown in Fig. 1(c).

3. Results and discussion

3.1. Effect of driving pulse (35 fs) intensity on HHG from silver plasma

3.1.1. Comparison of HHG spectra with ps LIPs and fs LIPs

Fig. 2(a–c) shows the 2D color plot of HHG spectra from fs LIPs of bulk and NPs (100 nm, 20 nm) with regard to change in DP intensities (I_{DP}), with a fixed $I_{HP} = 6.2 \times 10^{14}$ W/cm^2, respectively. The cut-off and intensity of harmonics are increased with growth in I_{DP}. It is observed that as the I_{DP} reaches 2.4 $\times$ 10^{14} W/cm^2 or higher, the spectrum possesses a plateau-like pattern from 13H to 55H. In general, plasma plumes commonly comprise atoms and different charge states of ions, contributing to HHG. The calculated harmonics spectra for silver within the range of $I_{DP} = 0.6$ to 4.8 $\times$ 10^{14} W/cm^2 were presented in our earlier work [16]. The results indicate that silver plasma components, i.e., atoms, Ag^+ and Ag^{2+} ions, are responsible for the generation of harmonics in three different ranges of I_{DP}, i.e., up to 1.2 $\times$ 10^{14} W/cm^2 Ag atoms and 1.2 to 1.8 $\times$ 10^{14} W/cm^2 range Ag^+ ions and higher than 1.8 $\times$ 10^{14} W/cm^2 Ag^{2+} ions are contributed towards the generation of harmonics. In the present case, the spectra shown in Fig. 2 with respect to different I_{DP} indicate that Ag atoms, Ag^+ enhance the harmonics between the harmonics orders 9H–17H, and 17H–41H, respectively. However, the total harmonics spectra, i.e., 9H–65H, mainly contribute from Ag^{2+} ions at higher I_{DP}.

Fig. 3 illustrates the theoretical cut-off of harmonics from Ag^+ ions (open circles) and Ag^{2+} ions (open upper triangles) and experimentally obtained cut-off for bulk and NPs in the case of fs LIPs and ps LIPs. The cut-off of ps LIP and theoretical ones is taken from Ref. [16] to compare with fs LIP. It was observed that for fs LIP, the order of the harmonics is extended. For example, at $I_{DP} = 0.6 \times 10^{14}$ W/cm^2 harmonic cut-off is almost equal to ps LIP data at I_{DP} 3.0 $\times$ 10^{14} W/cm^2 shown in Fig. 3 (mentioned by grey color square). It indicates that in the case of fs LIPs,

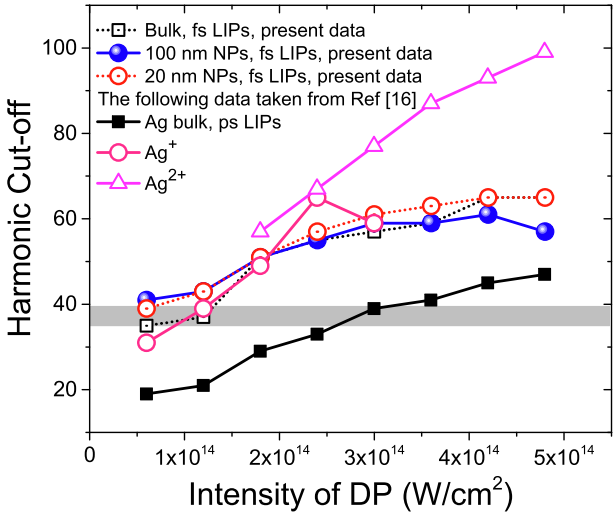

Fig. 3. Comparison of theoretical and experimental harmonic cut-off of bulk and NPs for fs HP (present study) and ps HP (earlier work [16]).

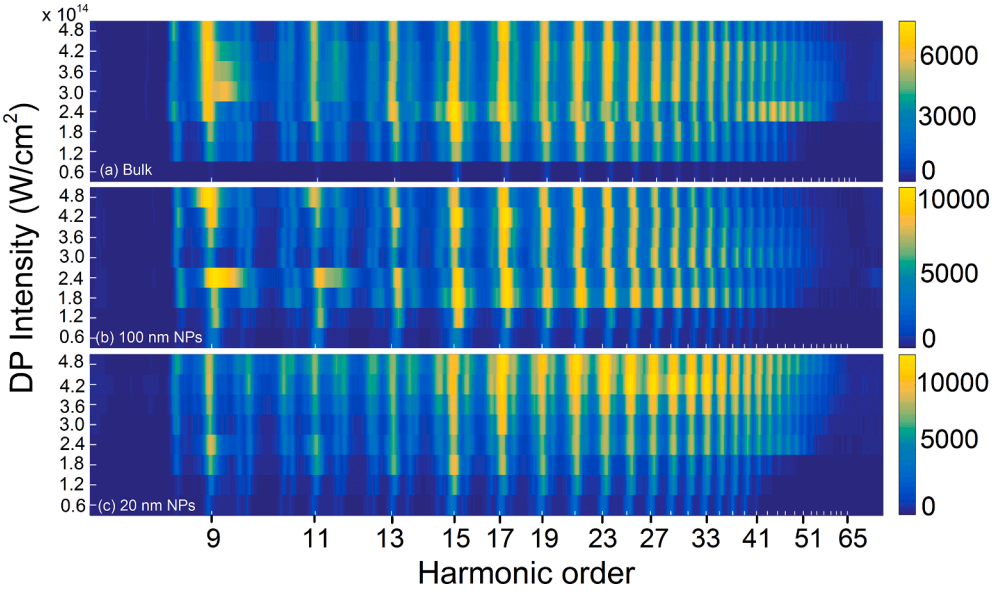

Fig. 2. HHG spectra at different intensities of the driving pulse (35 fs) for Ag (a) bulk and (b) 100 nm NPs and (c) 20 nm NPs.

the higher cut-off is achieved at lower I_{DP}. The exact cut-off was achieved for ps LIPs with higher I_{DP}, confirms that fs HP creates much denser plasma, with narrower angular distribution of ions. As per theoretical simulations, at 3.0×10^{14} W/cm^{2,} most harmonic spectra were generated from Ag^{2+} ions. But in the case of fs LIPs, this could be achieved at $I_{DP} = 0.6 \times 10^{14}$ W/cm^2 due to the high signal-to-noise ratio. As a result, the detector could show higher orders. The enhancement of signal-to-noise ratio and appearance of higher orders for fs LIPs has also confirmed a high density of plasma components than ps LIPs.

The comparison between the ns, ps and fs HPs experiments will reveal the change in the cut-off and intensity of harmonics majorly because the metal plasma plumes expansion/density in a vacuum varies to ablation laser pulse duration. The variation in the density of plasma plumes (consisting of atoms, ions and NPs) will affect the overall yield, cut-off order, and plateau pattern of harmonics. In our previous work [16], it is clear that the plasma plumes produced by ns pulses emit the stronger lower-order harmonics (9H–17H) than the higher-order range (more than 19H), whereas ps plasma plumes possessing intense harmonics throughout the harmonic spectra with cut-off up to 47H. However, in the present report, the harmonics cut-off for silver targets extended up to 65H. Fig. 4(a) shows the intensity of the maximum harmonic obtained by bulk and NPs of 100 nm and 20 nm sizes ablated by fs and ps laser pulses, respectively. It is observed that in the case of fs LIPs, the harmonics yield is stronger than ps LIPs.

Fig. 4(b) depicts the ratio of harmonics signals for fs LIPs to ps LIPs

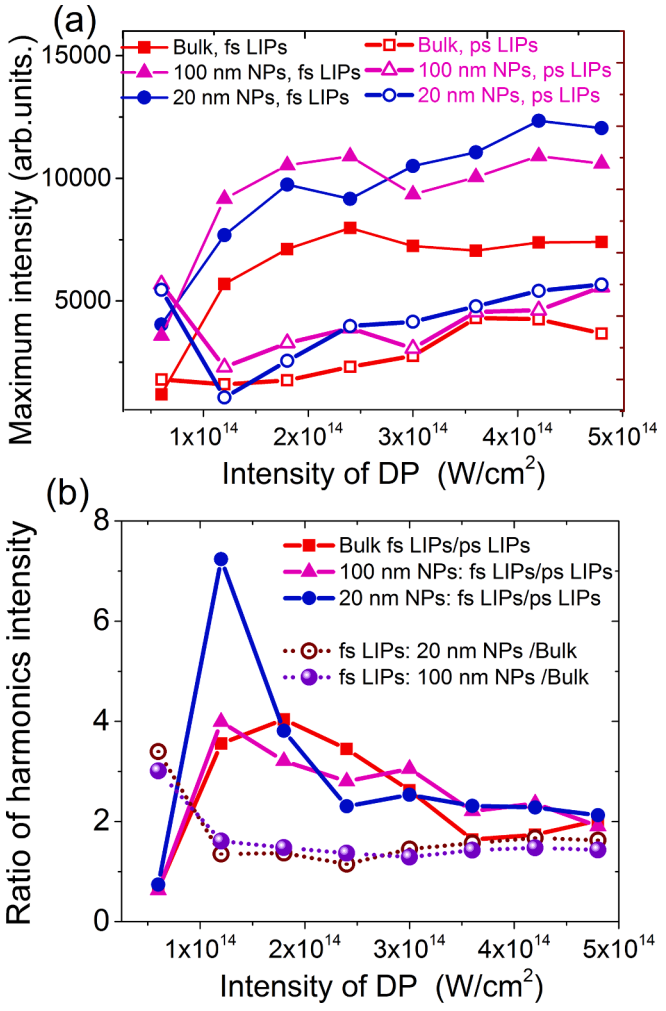

Fig. 4. (a) Maximum harmonic intensities for bulk and NPs, (b) ratio of harmonics signals for fs LIPs to ps LIPs and in case of fs LIPs; NPs to bulk for different intensities of DP.

for three targets and the ratio of NPs to bulk samples in the case of fs LIPs. The increment ratio is higher for NPs than bulk (please see subsection 3.1.2). The fs pulses intensities are 10^3 times higher than the ps HP intensities. Therefore, fs pulses might lead to the formation of free carriers and also increase the density of singly and double charges silver ions. It is expected that a high quantity of free electrons decreases the harmonics yield and cut-off. However, the experimental observations concerning fs laser ablation revealed that harmonics' intensity and cut-off are significantly improved compared to the ps laser ablation. Therefore, it is evidence that fs laser-induced plasma may also contain a high quantity of free electron density. Still, the presence of singly and doubly charged ions play a pivotal role in enhancing the harmonics cut-off and intensity. As shown in Fig. 3, the theoretically calculated harmonic cut-off for Ag^{2+} ions lies between the range of 55H–99H. But in experimental observations, the cut-off is achieved between the 37H–65H range. This decrement of cut-off might be due to the presence of a higher density of free electrons. However, the experimental harmonic cut-off for Ag+ is precisely matched with the theoretical cut-off in the present case. In Ag^{2+} ions, the experimental cut-off is ~1.3 times less than the theoretical cut-off.

Further, we have compared our results with earlier work on optimal ablating HPs intensity and achieved harmonic cut-offs. Ozaki et al. [42] and Bom et al. [43] studied individually the influence of the HP (τ_p = 210 ps) and I_{DP} on the harmonic spectrum using 20 TW, 10 Hz output of the ALLS laser from silver plasma plumes. This work mentioned that I_{HP} below and in the range of 1×10^{10} W/cm^2 are preferable to work for HHG from silver plasma and shown the appearance of doubly charged ions (Ag^{2+}) in the laser plume at the I_{HP} exceeding this level. This value they were estimated by calculating the electron density, ionization level and ion density with respect to different I_{HP} [43]. Also, in our earlier work [16], we have demonstrated the harmonics with emission with respect to ps HP below 1.2×10^{10} W/cm^2. In addition, Anatoly V. Andreev et al. presented the theoretical and experimental study of high-order optical harmonic generation in the ensemble of silver atoms irradiated using intense fs pulses of Ti: Sapphire laser. In this case, the HP has $\tau_p = 210$ ps and DP is obtained at $\lambda = 792$ nm at $\tau_p = 150$ fs. They have experimentally shown the harmonic cut-off from 9H to maximum cut-off up to 61H within the range of $I_{DP} = 1–10 \times 10^{14}$ W/cm^2. In the current results with fs HPs, the harmonic cut-off slightly exceeded compared to them. However, the harmonic cut-off in ps HP is closely matched with their results within the range of $I_{DP} = 1–4.8 \times 10^{14}$ W/cm^2. In brief, at $I_{DP} = 2.4 \times 10^{14}$ W/cm^2, they experimentally observed the harmonic cut-off up to 51 order. Our results (DP; $\tau_p = 35$ fs) are also closely matched and extended two orders more (i.e., 55H) with their results at the similar I_{DP}. Moreover, the harmonics became saturated in their studies at $I_{DP} = 3.5 \times 10^{14}$ W/cm^2. In the present case for fs LIPs, the harmonics became saturated for bulk silver around 3.0×10^{14} W/cm^2, as shown in Fig. 4(a).

3.1.2. Comparison of harmonics cut-off and yield for silver bulk and NPs (100 nm and 20 nm)

In most earlier studies, the cut-off in the case of the silver bulk was more significant than the one in the case of NPs of the same elemental state [20,21,44]. All those previous results where cut-off from bulk metal plasma was higher than from NPs were carried out using the ablation by ps and ns pulses. In the present report, we had ablated by silver targets (bulk, NPs) using fs pulses. We demonstrated the advanced feature when the evaporated NPs show the same properties as atoms and ions (from the point of cut-off) while maintaining the advanced features of NPs as better emitters of harmonics.

Figs. 2 and 3 show the cut-off of harmonics in the case of silver bulk, and NPs LIPs consistently show almost similar. It is known that LIPs from solids contain isolated atoms, ions (monomers), some clusters of atoms and NPs. The delay between HP and DP is fixed near 80 ns. Within this delay, the fast components (lower mass) could mainly contribute to the HHG. Therefore, it is anticipated that ablation of NPs containing targets

ejects a high quantity of smaller pieces than bulk, which also depends on the threshold of I_{HP}. However, we have ablated the three targets with the same I_{HP} and measured the harmonics spectra for different I_{DP}. Therefore, the similarity of cut-offs (shown in Fig. 3) might be including the specific regime of NPs ablation when some significant amount of atomic and ionic species of silver appears in the plasma plume due to the disintegration of NPs. The rate of deterioration can distinguish the processes of ablation of NPs by pulses of different durations. In the case of ablation of NPs by ns and ps pulses, the concentration of Ag atoms and ions is notably lower than in the case of application of the fs HPs. Correspondingly, those atoms and ions cause the generation of the same orders of harmonics, like in the case of ablation of the bulk target. In other words, in the case of fs plasma, there is a probability of achieving a more significant concentration of atoms and ions than the possibility of ns and ps HPs, which enhances the intensity of the harmonics.

This work observed that the NPs sample consistently gives a higher HHG yield (for most harmonic orders) than the bulk sample for different I_{DP}. In particular, at low I_{DP} 0.6 $\times$ 10^{14} W/cm^2, the intensity of harmonics for Ag 100 nm and 20 nm NPs is much more potent (~3 and 3.5 times) than bulk, as shown in Fig. 5. Also, the lower order harmonics, i.e., 9H,11H,13H, possess comparatively higher intensities for NPs than bulk. The cut-off of harmonics in the case of bulk and NPs LIPs, which steadily show a similar cut-off, where Ag 100 nm NPs show a little lower cut-off (shown in Figs. 2 and 3) than bulk, this result is identical to the earlier work. However, the harmonic yield is higher for NPs; among them, the smallest NPs show better efficiency as similar to earlier studies [13,20,21,44]. In brief, the smallest Ag 20 nm NPs show one odd-order higher cut-off at a lower I_{DP}, and the cut-off is matched for both bulk and smallest NPs cases at higher I_{DP} (4.2 and 4.8 $\times$ 10^{14} W/cm^2). However, the Ag 100 nm and 20 nm NPs possess some selected orders to have more substantial yield shown Fig. 2. The maximum harmonic signal is shown in Fig. 4(a) indicates that almost all the NPs plasmas have a higher yield than the bulk with respect to different I_{DP}.

The ablation of silver targets (bulk and NPs) certainly produces smaller NPs and clusters (small or high in size). The atoms inside the large NPs would hardly increase harmonic yield due to the absorption of XUV harmonics inside these species. However, the I_{HP} = 6.2 $\times$ 10^{14} W/cm^2 itself creates a larger amount of ions Ag^{+} (7.5762 eV) and Ag^{2+} (21.49 eV) during the ablation. Therefore, the probability of singly and doubly ionized atoms of silver for smaller NPs enhances the harmonics signal. In contrast, a small number of atoms could not affect the absorption of XUV harmonics.

Earlier, Ganeev et al. demonstrated the HHG from silver plasma ablated by ps laser pulses using fs DPs with different durations (also repetition rate). In their studies, the maximal order was achieved up to 13H–61H [20] and 21H–61H [33] and shown the intensity of the harmonics from bulk materials is higher than NPs composed targets. However, in our works, the plasma plumes created by ps and fs pulses have consistency with each other. i.e., the harmonic intensity is higher in the case of NPs than bulk, which is also supported by the same Ganeev et al. earlier works [2,45]. In our case, the recorded harmonics spectra starting with 9H, whereas earlier work starts from 13H, 15H and 21H, respectively. However, the determination of maximal generated order of harmonics depends on many experimental factors related to the detection of XUV pulses, including the wavelength, pulse duration, and pulse energy of driving and HPs, and delay between them.

3.2. Effect of chirped pulses on HHG

In this section, we have analyzed the harmonics spectra of bulk and NPs using negatively (−) and positively (+) chirped 135 fs pulses as DPs and compared with harmonic spectra recorded with chirp-free 35 fs pulses. Earlier, several research groups employed the HHG measurements from LIPs and gas molecules using DP with different durations [23–30]. In our laser system, it is impossible to obtain the different pulse durations with a similar central wavelength rather than changing the chirp of the pulses. The spectral profiles of chirp-free and chirped pulses were measured using a USB spectrometer (Ocean Optics) shown in Fig. 1 (b). All these pulses possess the same spectral components.

Meanwhile, their distribution along with the laser pulses significantly differs from each other. The blue and red components were equally distributed along with the temporal shape of chirp-free 35 fs pulses. It is well known that the blue and red components are moved towards the leading front and the tailing part of the pulses for negatively chirped pulses. In contrast, the blue and red components are moved towards the tailing position and leading front of the pulses for positively chirped pulses, respectively.

Fig. 6(a–c) shows the harmonic spectra from reported Ag bulk, 100

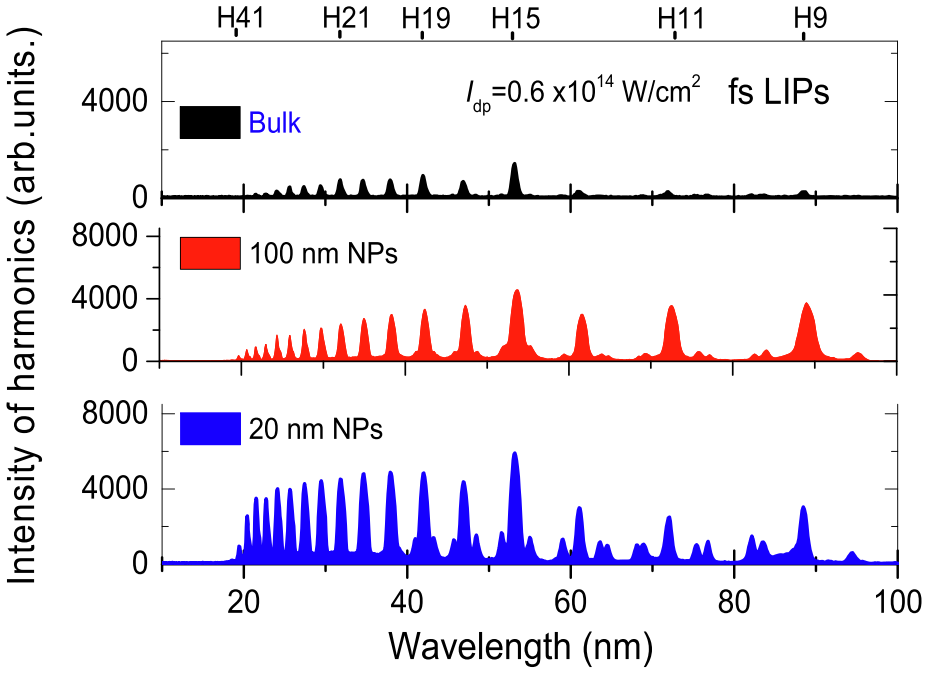

Fig. 5. HHG spectra of bulk and NPs at I_{DP} = 0.6 $\times$ 10^{14} W/cm^{2}for fs LIPs.

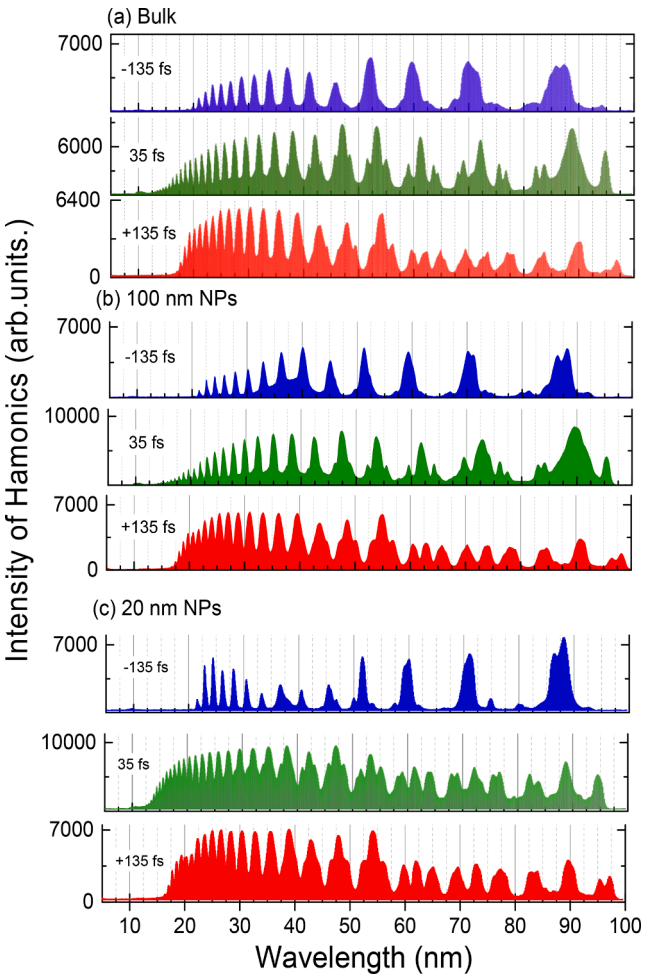

Fig. 6. HHG spectra for chirp-free 35 fs driving pulse [at 0.7 mJ (4.2×10^{14} W/cm^2)] and negative and positive chirps of 135 fs for (a) bulk, (b) 100 nm NPs and (c) 20 nm NPs, respectively.

nm and 20 nm NPs for chirp-free pulses of 35 fs, and with negatively (−) and positively (+) chirped 135 fs pulses, respectively. The laser peak intensity of the chirp-free 35 fs pulse was $I_{35fs} = 4.2 \times 10^{14}$ W/cm^2 (pulse energy 0.7 mJ), and the same laser pulse energy was used for chirped pulses. In bulk and NPs, harmonics up to the 65H orders were observed with chirp-free pulses. In the case of negatively chirped pulses, the harmonics became wider than positively chirped pulses. For example, in the case of bulk Ag, the measured full width at half of the maxima (FWHM) of 9H,11H,13H, and 15H are 3.9, 3.2, 2.2, and 1.9 nm for negatively chipped DP and 2.1, 1.5, 1.3, 1.1 nm for positively chirped DP. The broadening is decreased with an increase in the harmonic order. Also, the cut-off was reduced to 41H (bulk) and 35H (NPs) for negatively chirped DP. With positively chirped pulses, the harmonics in the plateau region (15H–37H) became sharp and strong, which is consistent with the earlier works [25,33]. The intensity of chirped pulses ($I_{135\ fs}$) decreased up to 0.9×10^{14} W/cm^2. As per energy cut-off law, [46] $E_{cut-off} = I_p + 3.17U_p$, where I_p is ionization potential; $U_p = 9.33 \times 10^{-14} I\,(W/cm^2)\,\lambda^2\,(\mu m)$ is the ponderomotive potential, in which I is the laser intensity at focus; and λ is the wavelength of the driving laser beam. The cut-off of harmonics is proportional to the driving laser intensity. The chirp-free pulses with shorter pulse duration have high peak intensities, leading to an increase in the cut-off. The harmonics cut-off and intensity were decreased compared to chirp-free pulses of 35 fs, as shown in Fig. 7(a, b). The harmonics spectra shifted towards shorter wavelengths (blueshift) and longer wavelengths (redshift) for negatively and positively chirped pulses, respectively (shown in Fig. 6).

Ganeev et al. explained the sources of spectral components for HHG using chirped pulses [33]. In brief, the leading edge of the chirped DP emits the harmonics. Therefore, it is expected that red and blue spectral components of positively and negatively chirped pulses emit the harmonics and possess corresponding redshift and blueshift in the harmonics compared to the chirp-free pulses harmonics spectra. In addition, it is observed that the chirped pulses enhance the different groups of harmonics even though they have the same peak intensities. This is due to variation in the distribution of spectral components, which are responsible for the generation of harmonics. As we mentioned above, in the case of positively chirped pulses, the red components, and negatively chirped pulses, the blue components are responsible for generating higher-order harmonics. As per energy cut-off law, [46] the cut-off of harmonics is proportional to the square of the driving laser wavelength. Therefore, under the similar intensity of chirped pulses, the increase in the wavelengths (red components, positive chirp) leads to an increased cut-off of harmonics. The decrease in the wavelengths (blue components, negative chirp) decreases the harmonics cut-off.

Fig. 6 shows the enhancement of different groups of harmonics with respect to chirped pulses. As earlier studies show in the case of silver plasma plumes; the higher-order harmonics possess stronger intensities than the lower range of harmonics [16,25,33]. Therefore, in the case of positively chirped pulses, the harmonics range 15H–37H shows a plateau-like pattern. Whereas due to a decrease in the wavelengths (blue components), the same peak intensity of laser pulses leads to enhance the lower order harmonics, i.e., 9H–15H. Moreover, the laser pulse frequency is time-dependent for chirped pulses, and the ratio between electric field and frequency can be assumed as a time-dependent function and which is given by Neyra et al. [29], followed by $U^*(t) = \frac{E(t)^2}{4\omega(t)^2}$.

The values of $U^*(t)$ might have less/equal/ higher than the ponderomotive potential (U_p) for specific time intervals Δt, and which given by$\Delta t = \frac{E(t)^2}{4U_p} - \omega(t)^2$. If the time interval ($\Delta t$) is negative or positive, then the corresponding time-dependent for ponderomotive potential is lower or higher than the U_P. Subsequently, in negatively chirped pulses, the extension of harmonics is not possible due to negative time intervals. Whereas, for positively chirped pulses, the positive values of time intervals are higher than actual U_p, which leads to an extension of cut-off. Our HHG measurements support this phenomenon in the case of three samples shown in Fig. 6. However, the cut-off could not be exceeded for positively chirped pulses than chirp-free pulses due to the lower peak intensity of DP. Fig. 8 depicts the 2D color map of HHG spectra for bulk sample (data taken from Fig. 6(a)) for negatively and positively chirped 135 fs pulses. The harmonic spectra extended up to 47H for positive chirp DP than negative chirp DP (41H). It was also observed that the harmonics 15H to 45H are stronger than 9H, 11H, and 13H for positively chirped pulses. In contrast, the lower order harmonics, i.e., 9H to 15H, are more substantial than 17H to 41H for negatively chirped pulses.

Overall, the presented results indicated that Ag is one of the prominent materials for emission sources of higher-order harmonics. The intensity and cut-off of harmonics could be preciously tuned with respect to driving and heating pulse durations and intensities.

4. Conclusions

In summary, we have presented higher-order harmonics from LIPs of silver ablated by fs HP. The shorter pulse duration of HP leads to an increase in the plasma density. Consequently, it improves the higher quantity of ions with a narrower angular distribution. As a result, the harmonic cut-off is precisely matched with Ag^+ ions and almost 1.3 times less than the Ag^{2+} ions contribution of theoretically calculated HHG spectra. It is also noticed that the harmonic cut-off and intensities are higher for NPs than bulk. In addition, the chirped pulses lead to redshift and blueshift of harmonics corresponding to positively and negatively chirped DPs. The positively chirped pulses increase the

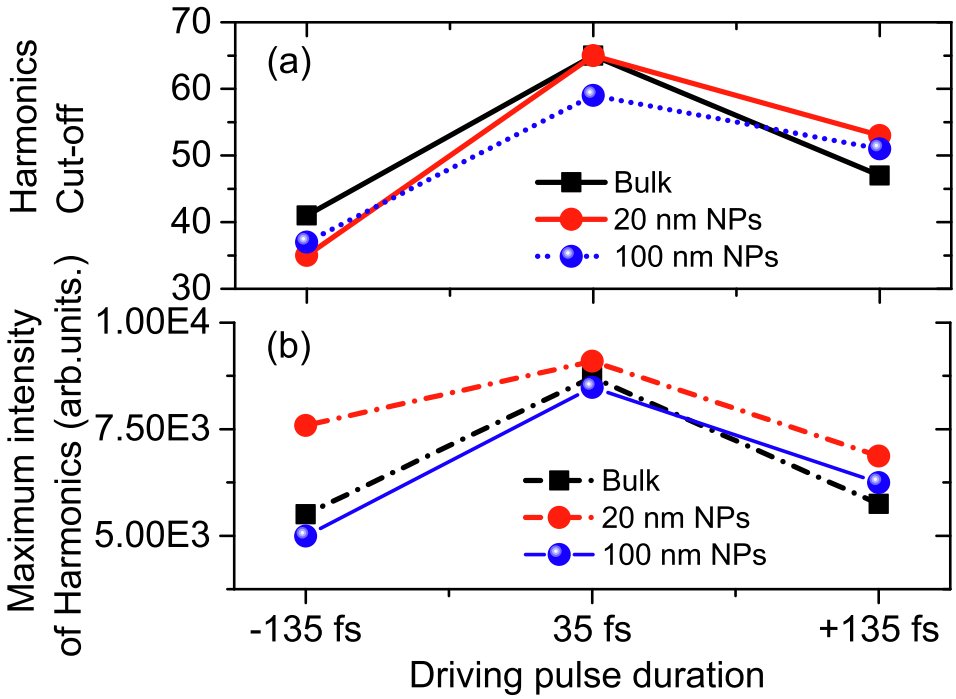

Fig. 7. (a) Harmonic cut-off and (b) intensity of harmonics for driving pulses of chirp-free 35 fs pulses and negatively (−) and positively (+) chirped 135 fs pulses.

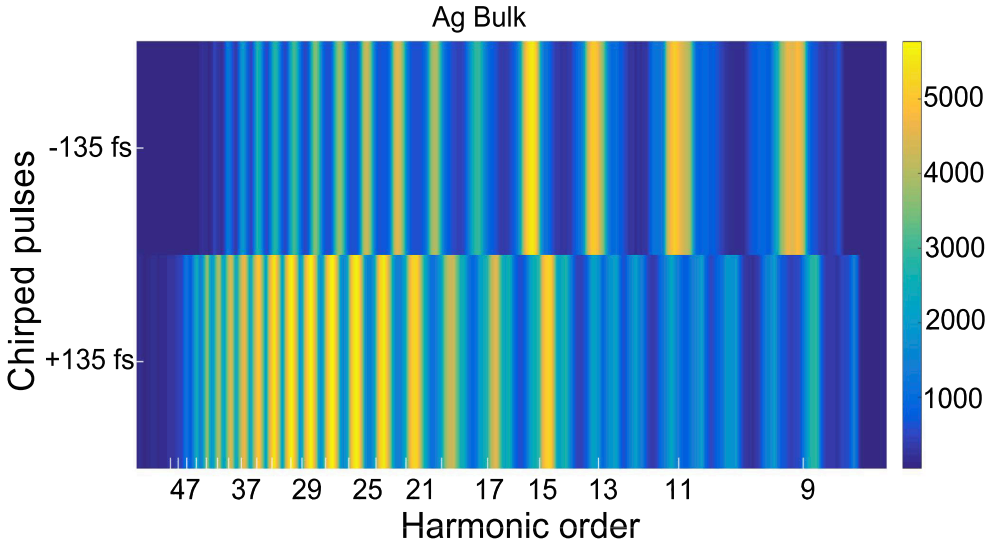

Fig. 8. HHG spectra of bulk Ag at driving pulses of negatively (−) and positively (+) chirped 135 fs pulses.

harmonic cut-off with higher intensities of higher-order harmonics 15H to 41H, whereas for negatively chirped pulses, the lower order 9H to 15H intensities are higher than the higher-order range, i.e., 17H to 35H. In our earlier work [16], we have compared the HHG spectra of Ag bulk and 20 nm NPs in the case of ps LIPs and ns LIPs. The present study opens a new channel for the ablation of materials with fs pulses to create the denser plasma. Further, it leads to high conversion efficiency and cut-off of harmonics which can be used for the next generation of table-top XUV radiation sources.

CRediT authorship contribution statement

Srinivasa Rao Konda: Conceptualization, Writing – original draft, Methodology, Software, Investigation, Writing – review & editing. **Yu Hang Lai:** Software, Writing – review & editing. **Wei Li:** Writing – review & editing, Supervision, Project administration, Funding acquisition.

Declaration of Competing Interest

The authors declare that they have no known competing financial interests or personal relationships that could have appeared to influence the work reported in this paper.

Acknowledgements

Srinivasa Rao Konda acknowledges support by the Chinese Academy of Sciences President's International Fellowship Initiative [grant no. 2021PM0036]. This work is supported by The Innovation Grant of Changchun Institute of Optics, Fine Mechanics and Physics (CIOMP),

Jilin Provincial Science and Technology Development Project [grant no. YDZJ202102CXJD002], Development Program of the Science and Technology of Jilin Province, 20200802001GH, and the National Natural Science Foundation of China [grant no. 12004380].

References

[1] R.A. Ganeev, M. Suzuki, M. Baba, M. Ichihara, H. Kuroda, Low- and high-order nonlinear optical properties of Au, Pt, Pd, and Ru nanoparticles, J. Appl. Phys. 103 (6) (2008) 063102, https://doi.org/10.1063/1.2887990.

[2] R.A. Ganeev, Harmonic generation from partially ionized plasma [Invited], J. Opt. Soc. Am. B. 31 (9) (2014) 2221, https://doi.org/10.1364/JOSAB.31.002221.

[3] H. Singhal, P.A. Naik, M. Kumar, J.A. Chakera, P.D. Gupta, Enhanced coherent extreme ultraviolet emission through high order harmonic generation from plasma plumes containing nanoparticles, J. Appl. Phys. 115 (3) (2014) 033104, https://doi.org/10.1063/1.4862302.

[4] M.A. Fareed, V.V. Strelkov, N. Thiré, S. Mondal, B.E. Schmidt, F. Légaré, T. Ozaki, High-order harmonic generation from the dressed autoionizing states, Nat. Commun. 8 (2017) 16061, https://doi.org/10.1038/ncomms16061.

[5] L.B. Elouga Bom, S. Haessler, O. Gobert, M. Perdrix, F. Lepetit, J.-F. Hergott, B. Carré, T. Ozaki, P. Salières, Attosecond emission from chromium plasma, Opt. Express 19 (2011) 3677–3685, https://doi.org/10.1364/OE.19.003677.

[6] Y. Pertot, S. Chen, S.D. Khan, L.B.E. Bom, T. Ozaki, Z. Chang, Generation of continuum high-order harmonics from carbon plasma using double optical gating, J. Phys. B At. Mol. Opt. Phys. 45 (7) (2012) 074017, https://doi.org/10.1088/0953-4075/45/7/074017.

[7] N. Rosenthal, G. Marcus, Discriminating between the Role of Phase Matching and that of the Single-Atom Response in Resonance Plasma-Plume High-Order Harmonic Generation, Phys. Rev. Lett. 115 (2015), 133901, https://doi.org/10.1103/PhysRevLett.115.133901.

[8] M. Venkatesh, R.A. Ganeev, K.S. Rao, G.S. Boltaev, K.e. Zhang, A. Srivastava, J. K. Bindra, S. Singh, V.V. Kim, S.K. Maurya, G.F. Strouse, N.S. Dalal, C. Guo, In fl uence of gadolinium doping on low- and high-order nonlinear optical properties and transient absorption dynamics of ZnO nanomaterials, Opt. Mater. (Amst) 95 (2019) 109241, https://doi.org/10.1016/j.optmat.2019.109241.

[9] R.A. Ganeev, G.S. Boltaev, V.V. Kim, M. Iqbal, H. Kuroda, A.S. Alnaser, Distinction in resonance properties of the atomic and molecular contained plasmas used for high-order harmonics generation of ultrafast laser pulses, J. Appl. Phys. 129 (4) (2021) 043103, https://doi.org/10.1063/5.0034861.

[10] R.A. Ganeev, S. Odžak, D.B. Milošević, M. Suzuki, H. Kuroda, Resonance enhancement of harmonics in metal plasmas using tunable mid-infrared pulses, Laser Phys. 26 (7) (2016) 075401, https://doi.org/10.1088/1054-660X/26/7/075401.

[11] R.A. Ganeev, T. Witting, C. Hutchison, V.V. Strelkov, F. Frank, M. Castillejo, I. Lopez-Quintas, Z. Abdelrahman, J.W.G. Tisch, J.P. Marangos, Comparative studies of resonance enhancement of harmonic radiation in indium plasma using multicycle and few-cycle pulses, Phys. Rev. A 88 (2013) 33838, https://doi.org/10.1103/PhysRevA.88.033838.

[12] R.A. Ganeev, M. Suzuki, S. Yoneya, H. Kuroda, High-order harmonic generation during propagation of femtosecond pulses through the laser-produced plasmas of semiconductors, J. Appl. Phys. 117 (023114) (2015) 1–8, https://doi.org/10.1063/1.4905902.

[13] J.A. Chakera, H. Singhal, R.A. Ganeev, P.A. Naik, A.K. Srivastav, A. Singh, R. Chari, A. Khan, P.D. Gupta, Higher Harmonic Generation Using Nano-structured Target Plumes, AIP Conf. Proc. 1228 (2010) 413, https://doi.org/10.1063/1.3426082.

[14] M. Masnavi, M. Nakajima, K. Horioka, H.P. Araghy, A. Endo, Simulation of particle velocity in a laser-produced tin plasma extreme ultraviolet source, J. Appl. Phys. 109 (12) (2011) 123306, https://doi.org/10.1063/1.3601346.

[15] R.A. Ganeev, G.S. Boltaev, V.V. Kim, M. Venkatesh, A.I. Zvyagin, M.S. Smirnov, O. V. Ovchinnikov, M. Wöstmann, H. Zacharias, C. Guo, High-order harmonic generation using quasi- phase matching and two-color pump in the plasmas containing molecular and alloyed metal sulfide quantum dots, J. Appl. Phys. 126 (19) (2019) 193103, https://doi.org/10.1063/1.5124139.

[16] S.R. Konda, Y.H. Lai, W. Li, Investigation of high harmonic generation from laser ablated plumes of silver, J. Appl. Phys. 130 (1) (2021) 013101, https://doi.org/10.1063/5.0054337.

[17] R.A. Ganeev, M. Suzuki, M. Baba, H. Kuroda, High-order harmonic generation from laser plasma produced by pulses of different duration, Phys. Rev. A 76 (2007), 023805, https://doi.org/10.1103/PhysRevA.76.023805.

[18] R.A. Ganeev, M. Baba, M. Suzuki, H. Kuroda, High-order harmonic generation from silver plasma, Phys. Lett. A 339 (2005) 103–109, https://doi.org/10.1016/j.physleta.2005.02.073.

[19] R.A. Ganeev, L.B. Elouga Bom, T. Ozaki, Comparison of high-order harmonic generation from various cluster- and ion-containing laser plasmas, J. Phys. B At. Mol. Opt. Phys. 42 (5) (2009) 055402, https://doi.org/10.1088/0953-4075/42/5/055402.

[20] R.A. Ganeev, M. Suzuki, M. Baba, M. Ichihara, H. Kuroda, High-order harmonic generation in Ag nanoparticle-containing plasma, J. Phys. B At. Mol. Opt. Phys. 41 (4) (2008) 045603, https://doi.org/10.1088/0953-4075/41/4/045603.

[21] H. Singhal, R.A. Ganeev, P.A. Naik, A.K. Srivastava, A. Singh, R. Chari, R.A. Khan, J.A. Chakera, P.D. Gupta, Study of high-order harmonic generation from nanoparticles, J. Phys. B At. Mol. Opt. Phys. 43 (2) (2010) 025603, https://doi.org/10.1088/0953-4075/43/2/025603.

[22] B. Verhoff, S.S. Harilal, J.R. Freeman, P.K. Diwakar, A. Hassanein, Dynamics of femto- and nanosecond laser ablation plumes investigated using optical emission spectroscopy, J. Appl. Phys. 112 (9) (2012) 093303, https://doi.org/10.1063/1.4764060.

[23] X. Feng, S. Gilbertson, H. Mashiko, H. Wang, S.D. Khan, M. Chini, Y. Wu, K. Zhao, Z. Chang, Generation of Isolated Attosecond Pulses with 20 to 28 Femtosecond Lasers, Phys. Rev. Lett. 103 (2009), 183901, https://doi.org/10.1103/PhysRevLett.103.183901.

[24] K. Légaré, R. Safaei, G. Barrette, L. Arias, P. Lassonde, H. Ibrahim, B. Vodungbo, E. Jal, J. Lüning, N. Jaouen, Z. Tao, A. Baltuška, F. Légaré, G. Fan, Raman Red-Shift Compressor: A Simple Approach for Scaling the High Harmonic Generation Cut-Off, Adv. Photonics Res. (2021) 2100113, https://doi.org/10.1002/adpr.202100113.

[25] D.G. Lee, J.H. Kim, K.H. Hong, C.H. Nam, Coherent control of high-order harmonics with chirped femtosecond laser pulses, Phys. Rev. Lett. 87 (2001) 2439021–2439024, https://doi.org/10.1103/PhysRevLett.87.243902.

[26] V. Tosa, H.T. Kim, I.J. Kim, C.H. Nam, High-order harmonic generation by chirped and self-guided femtosecond laser pulses. I. Spatial and spectral analysis, Phys. Rev. A 71 (2005) 1–7, https://doi.org/10.1103/PhysRevA.71.063807.

[27] J.-X. Han, J. Wang, Y. Qiao, A.-H. Liu, F.-M. Guo, Y.-J. Yang, Significantly enhanced conversion efficiency of high-order harmonic generation by introducing chirped laser pulses into scheme of spatially inhomogeneous field, Opt. Express 27 (6) (2019) 8768, https://doi.org/10.1364/OE.27.008768.

[28] J.-G. Fan, X.-Y. Miao, X.-F. Jia, Control of the high-order harmonic generation by sculpting waveforms with chirp in solids, Chem. Phys. Lett. 762 (2021) 138136, https://doi.org/10.1016/j.cplett.2020.138136.

[29] E. Neyra, F. Videla, J.A. Pérez-Hernández, M.F. Ciappina, L. Roso, G.A. Torchia, High-order harmonic generation driven by chirped laser pulses induced by linear and non linear phenomena, Eur. Phys. J. D 70 (2016) 2–8, https://doi.org/10.1140/epjd/e2016-70320-5.

[30] C.X. Yun, H. Teng, W. Zhang, M.J. Zhan, H.N. Han, X. Zhong, Z.Y. Wei, B.B. Wang, X. Hou, High-order harmonics generation by few-cycle and multi-cycle femtosecond laser pulses, Chinese Phys. B 19 (2010) 1–4, https://doi.org/10.1088/1674-1056/19/12/124210.

[31] F. Lu, Y. Xia, S. Zhang, D. Chen, High-order harmonic generation from Xe-Ar gas mixture in the tight focusing laser, Opt. Laser Technol. 57 (2014) 145–148, https://doi.org/10.1016/j.optlastec.2013.10.011.

[32] J.-K. An, K.-H. Kim, Efficient non-perturbative high-harmonic generation from nonlinear metasurfaces with low pump intensity, Opt. Laser Technol. 135 (2021) 106702, https://doi.org/10.1016/j.optlastec.2020.106702.

[33] R.A. Ganeev, H. Singhal, P.A. Naik, U. Chakravarty, V. Arora, J.A. Chakera, R. A. Khan, M. Raghuramaiah, S.R. Kumbhare, R.P. Kushwaha, P.D. Gupta, Optimization of the high-order harmonics generated from silver plasma, Appl. Phys. B Lasers Opt. 87 (2) (2007) 243–247, https://doi.org/10.1007/s00340-007-2583-0.

[34] R.A. Ganeev, Enhancement of high-order harmonics generated in laser-produced plasma using ionic resonances and nanoparticles, Opt. Spectrosc. 122 (2) (2017) 250–268, https://doi.org/10.1134/S0030400X17010076.

[35] S. Hadrich, M. Krebs, A. Hoffmann, A. Klenke, J. Rothhardt, J. Limpert, A. Tu, Exploring new avenues in high repetition rate table-top coherent extreme ultraviolet sources, Light Sci. Appl. 4 (2015) e320, https://doi.org/10.1038/lsa.2015.93.

[36] J. Li, J. Lu, A. Chew, S. Han, J. Li, Y. Wu, H. Wang, S. Ghimire, Z. Chang, Attosecond science based on high harmonic generation from gases and solids, Nat. Commun. 11 (2020) 2748, https://doi.org/10.1038/s41467-020-16480-6.

[37] N. Kanda, T. Imahoko, K. Yoshida, A. Tanabashi, A. Amani Eilanlou, Y. Nabekawa, T. Sumiyoshi, M. Kuwata-Gonokami, K. Midorikawa, Opening a new route to multiport coherent XUV sources via intracavity high-order harmonic generation, Light Sci. Appl. 9 (2020) 168, https://doi.org/10.1038/s41377-020-00405-5.

[38] Z. Chen, M. Segev, Highlighting photonics: looking into the next decade, ELight 1 (2021) 1–12, https://doi.org/10.1186/s43593-021-00002-y.

[39] S.R. Konda, V.R. Soma, M. Banavoth, R. Ketavath, V. Mottamchetty, Y.H. Lai, W. Li, High Harmonic Generation from Laser-Induced Plasmas of Ni-Doped CsPbBr 3 Nanocrystals: Implications for Extreme Ultraviolet Light Sources, ACS Appl. Nano Mater. 4 (8) (2021) 8292–8301, https://doi.org/10.1021/acsanm.1c01490.

[40] Y.H. Lai, K.S. Rao, J. Liang, X. Wang, C. Guo, W. Yu, W. Li, Resonance-enhanced high harmonic in metal ions driven by elliptically polarized laser pulses, Opt. Lett. 46 (2021) 2372–2375, https://doi.org/10.1364/OL.425495.

[41] R.A. Rajan, C.-V. Ngo, J. Yang, Y.u. Liu, K.S. Rao, C. Guo, Femtosecond and picosecond laser fabrication for long-term superhydrophilic metal surfaces, Opt. Laser Technol. 143 (2021) 107241, https://doi.org/10.1016/j.optlastec.2021.107241.

[42] T. Ozaki, L.B. Elouga Bom, R. Ganeev, J.-C. Kieffer, M. Suzuki, H. Kuroda, Intense harmonic generation from silver ablation, Laser Part. Beams 25 (2) (2007) 321–325, https://doi.org/10.1017/S0263034607000201.

[43] L.B. Elouga Bom, J.C. Kieffer, R.A. Ganeev, M. Suzuki, H. Kuroda, T. Ozaki, Influence of the main pulse and prepulse intensity on high-order harmonic generation in silver plasma ablation, Phys. Rev. A 75 (2007) 1–8, https://doi.org/10.1103/PhysRevA.75.033804.

[44] T. Ozaki, L.B. Elouga Bom, J. Abdul-Hadi, R.A. Ganeev, Evidence of strong contribution from neutral atoms in intense harmonic generation from

nanoparticles, Laser Part. Beams 28 (1) (2010) 69–74, https://doi.org/10.1017/S0263034609990589.
[45] R.A. Ganeev, C. Hutchison, I. Lopez-Quintas, F. McGrath, D.Y. Lei, M. Castillejo, J. P. Marangos, Ablation of nanoparticles and efficient harmonic generation using a 1-kHz laser, Phys. Rev. A 88 (3) (2013), https://doi.org/10.1103/PhysRevA.88.033803.
[46] P.B. Corkum, Plasma perspective on strong field multiphoton ionization, Phys. Rev. Lett. 71 (13) (1993) 1994–1997, https://doi.org/10.1103/PhysRevLett.71.1994.